Smart Structures and Systems, *Vol. 28, No. 5 (2021) 675-687*
https://doi.org/10.12989/sss.2021.28.5.675

Structural instantaneous frequency extraction based on improved multi-synchrosqueezing generalized S-transform

Ping-Ping Yuan [1,2,3a], Xue-Li Cheng [4b], Hang-Hang Wang [3c], Jian Zhang*[4], Zhong-Xiang Shen [3d] and Wei-Xin Ren [5e]

[1] *School of Materials Science and Engineering, Jiangsu University of Science and Technology, Zhenjiang, 212100, Jiangsu, China*
[2] *Jiangsu New Yangzi Shipbuilding Co., Ltd., Jingjiang, 214532, Jiangsu, China*
[3] *School of Civil Engineering and Architecture, Jiangsu University of Science and Technology, Zhenjiang, 212100, Jiangsu, China*
[4] *School of Naval Architecture and Ocean Engineering, Jiangsu University of Science and Technology, Zhenjiang, 212100, Jiangsu, China*
[5] *College of Civil and Transportation Engineering, Shenzhen University, Shenzhen, 518060, Guangdong, China*

(*Received February 9, 2021, Revised June 29, 2021, Accepted August 3, 2021*)

Abstract. A new method is proposed to improve the accuracy of structural instantaneous frequency (IF) extraction. The proposed method combines a new form of improved generalized S-transform (IGST) and a multi-synchrosqueezing operation. The parameters selection of the window function in IGST is derived through the concentration measure (CM) principle. Then, the multi-synchrosqueezing algorithm is employed to improve energy aggregation of time-frequency analysis (TFA). To verify the effectiveness and accuracy of the proposed improved multi-synchrosqueezing generalized S-transform (IMSSGST), a frequency-modulated multi-component signal is investigated. For structural IF extraction, a two-story shear frame and a three-story steel frame structure are introduced. Furthermore, the IF identification of a seven-story RC shear wall structure is conducted to verified the practicability in actual engineering. Numerical simulation and experimental results show that the proposed method can effectively improve the energy aggregation of TFA and effectively improve the accuracy of IF identification.

Keywords: concentration measure; improved multi-synchrosqueezing generalized S-transform; improved generalized S-transform; instantaneous frequency; time-frequency analysis

1. Introduction

With the development of society, the role of civil engineering structures in daily life is becoming more and more important. Structural damage will inevitably lead to the change of structural dynamic characteristics. With the accumulation of damage, once there is a problem, it will cause property losses and affect people's normal life. What's worse, it will cause casualties. The structural dynamic characteristics often change over time during their service life. Therefore, for these time-varying structures, it is of great significance to accurately extract time-dependent dynamic parameters such as instantaneous frequencies and instantaneous amplitudes, which will benefit for health monitoring, damage identification and safety assessment of engineering structures (Kijewski and Kareem 2003, Liu *et al*. 2015, Thakur and Wu 2011). The response signals of time-varying or nonlinear structures are often non-stationary, which creates challenge to traditional linear methods. As a new signal processing method, TFA is an important and widely accepted tool to deal with non-stationary signals. By designing the joint function of time and frequency, time-frequency signals can be transformed into a two-dimensional plane, thus reflecting energy and intensity in both time domain and frequency domain. Although many researches have demonstrated that TFA could be an ideal solution for non-stationary signals, all traditional TFA methods such as short-time Fourier transform (STFT), Winger-Ville distribution (WVD), S-transform (ST), Hilbert-Huang transform (HHT) have some shortcomings (Wang *et al*. 2018). For example, the empirical mode decomposition (EMD) in HHT is not guaranteed theoretically and it's inapplicable for the decomposition of closely-spaced frequency components (Lei *et al*. 2013).

In general, the ST uses a Gaussian window, whose standard deviation varies with frequency. No matter what signal is analyzed, the width of the Gaussian window will decrease with the increase of frequency. This results in a higher frequency resolution at lower frequencies and a higher time resolution at higher frequencies (Moukadem *et al*. 2015). Based on this imperfection, many scholars have further carried out relevant research. A time-varying modal parameter identification method based on linear time-frequency representation and Hilbert transform (HT) was

*Corresponding author, Professor,
E-mail: justzj@just.edu.cn
[a] Ph.D., E-mail: yuanpingping@just.edu.cn
[b] Graduate Student, E-mail: xueli_c@126.com
[c] Graduate Student, E-mail: justwanghh@163.com
[d] Ph.D., E-mail: zhongxiang-shen@just.edu.cn
[e] Professor, E-mail: renwx@szu.edu.cn

ISSN: 1738-1584 (Print), 1738-1991 (Online)

proposed. With Gabor expansion and synthesis, measured responses were represented in time-frequency domain and the modal components were reconstructed by time-frequency filtering (Xu *et al*. 2003). Pinnergar and Mansinha (2003) proposed another GST in which two prescribed functions of frequency control the scale and the shape of the analyzing window, and applied it to determining P-wave arrival time in a noisy seismogram. Djurović *et al*. (2008) put forward a modified ST to enhance the energy concentration in time-frequency domain. Assous and Boashash (2012) considered the problem of phase synchrony and coherence analysis using a modified version of the ST (MST). This basic method includes a cross-spectral analysis to study the phase synchrony of non-stationary signals, and relies on some properties of the MST, such as phase preservation. Liu *et al*. (2017a applied a three parameters ST to time-frequency analysis of seismic data. Later, a self-adaptive generalized S-transform was put forward again for seismic time–frequency analysis by Liu *et al*. (2019). Damage identification of high-rise frame structures based on STFT was presented by Guo and Pei (2017). Zidelmal *et al*. (2017) proposed an S-transform based on compact support kernel (CSK). This method used a CSK instead of the Gaussian window and the width of CSK is controlled by parameters making it more flexible.

As an adaptive operation, wavelet transform (WT) is particularly used for analyzing non-stationary transient signals (Ni *et al*. 2017, Patil and Hamde 2021). In the past three decades, it has achieved great success in parameter identification and damage detection of time-varying or nonlinear structures. For example, Hou *et al*. (2010) presented an instantaneous modal parameter identification method of earthquake excited structures based on continuous wavelet transform (CWT). In fact, CWT can realize signal transformation and reconstruction, and keep the consistency and reversibility of original information. However, the responses measured in environmental vibration test are often mixed with harmonic components, so that the CWT cannot be used directly. To solve this problem, Le and Argoul (2015) proposed a time-frequency domain decomposition technique to distinguish harmonic components from structural modes in the operational modal identification. Zheng *et al*. (2017) presented an adaptive parameter-less empirical wavelet transform based TFA method and applied it to rotor rubbing fault diagnosis. Combining maximum gradient and smoothing operation, Liu *et al*. (2018a) proposed a new method for IF extraction in time-varying structures. The results demonstrated that the proposed method can extract instantaneous frequencies from the noisy multi-component signals and practical response signals successfully.

Theoretically, the energy of a response signal concentrates around several curves in the time-frequency plane after CWT is performed. To further improve the energy aggregation, Daubechies *et al*. (2011) proposed the synchrosqueezed wavelet transform (SWT) based on WT. This method effectively improved the energy concentration by squeezing the energy around time-frequency. Furthermore, Liu *et al*. (2015) used SWT to detect structural time-varying damage. Zhang *et al*. (2018) applied SWT to the extraction of instantaneous attributes of seismic signals. Liu *et al*. (2017b, 2018b) used synchrosqueezing transform to study high-resolution characterization of geologic structures and applied SST-MAW to seismic instantaneous frequency extraction. The SWT algorithm redistributes energy in the frequency direction to suppress the ambiguity along the frequency axis, but it cannot achieve good resolution in the time domain. Li and Liang (2012) proposed a generalized synchrosqueezing transform (GST) method to enhance signal time-frequency representation, but this algorithm can only work well when the phase function or modulation source of the frequency modulated signal is known in advance. Pham and Meignen (2017) proposed a high-order synchrosqueezing transform for multi-component signals analysis. More researches about SWT and its improvements can be found in the references (Feng *et al*. 2015, Oberlin *et al*. 2015, Cao *et al*. 2016, Behera *et al*. 2018, Sanchez *et al*. 2020).

Inspired by SWT algorithm, Yu *et al*. (2017) put forward a new TFA method, namely synchroextracting transform (SET), to study the trend and IF of nonlinear and non-stationary data. This method is a postprocessing procedure of STFT, which can generate a more energy concentrated representation and improve accuracy of IF. Kang (2018) systematically studied the application and improvement of SET for seismic signal analysis. Zhang *et al*. (2020) further proposed a gas turbine order tracking method based on SET and Vold-Kalman filter. Li *et al*. (2020) proposed a time-synchroextracting generalized Chirplet transform for seismic TFA. However, SET cannot achieve accurate signal reconstruction, so, Yu *et al*. (2019) further proposed multi-synchrosqueezing Transform (MSST). In fact, this method performed multiple synchrosqueezing processing on the time-frequency image obtained by STFT to effectively improve the energy aggregation.

To further enhance the accuracy of IF extraction from structural non-stationary responses, we presented an improved multi-synchrosqueezing generalized S-transform (IMSSGST) based on IGST and MSST. In this method, the window function of GST was improved, and the parameters of window function were selected according to the centration measure (CM) principle (Stanković 2001). The MSST was then introduced to perform multiple synchrosqueezing processing. In the aspect of numerical simulation, a frequency-modulated multi-component signal was investigated. For structural IF extraction, a two-story shear frame model and a three-story steel frame structure were also introduced. In terms of experiment, the IF identification of a seven-story RC shear wall structure is conducted to verified the practicability in actual engineering. Numerical simulation and experimental results show that the proposed method can effectively improve the energy aggregation of TFA and effectively improve the accuracy of IF identification.

The outline of this paper is arranged as follows. The new IMSSGST is proposed in detail in Section 2. A frequency-modulated multi-component signal is presented in Section 3 to illustrate the proposed method. Two numerical examples of structural IF extractions are

introduced in Section 4, followed by an experimental demonstration on a seven-story RC shear wall structure in Section 5. The evaluation outcomes are summarized in conclusion section at the end of this paper.

2. Improved multi-synchrosqueezing generalized S-transform

2.1 Improved generalized S-transform

ST is a TFA method combining STFT and CWT, which is characterized by introducing a Gaussian window whose width is inversely proportional to frequency. The transform is defined as

$$S(\tau,f)=\int_{-\infty}^{+\infty}x(t)g(t-\tau)e^{-i2\pi f t}dt \tag{1}$$

where $x(t)$ is original signal, $g(t)$ is a window function, τ is the time shift factor, and f is frequency. The expression of $g(t)$ is shown in Eq. (2)

$$g(t)=\frac{|f|}{\sqrt{2\pi}}e^{\frac{-t^2f^2}{2}} \tag{2}$$

Thus, ST can be expressed as follows

$$S(\tau,f)=\frac{|f|}{\sqrt{2\pi}}\int_{-\infty}^{+\infty}x(t)e^{\frac{-(t-\tau)^2f^2}{2}}e^{-i2\pi f t}dt \tag{3}$$

Additionally, ST has complete reversibility, and its inverse transformation is shown in Eq. (4)

$$x(t)=\int_{-\infty}^{+\infty}\left[\int_{-\infty}^{+\infty}S(\tau,f)d\tau\right]e^{i2\pi f t}df \tag{4}$$

In ST, let

$$g(t)=\frac{\lambda|f|^p}{\sqrt{2\pi}}e^{\frac{-\lambda^2t^2f^{2p}}{2}} \tag{5}$$

The classical GST can be obtained and expressed by the following formula

$$GST(\tau,f)=\int_{-\infty}^{+\infty}x(t)\frac{\lambda|f|^p}{\sqrt{2\pi}}e^{\frac{-\lambda^2f^{2p}(t-\tau)^2}{2}}e^{-i2\pi f t}dt \tag{6}$$

To further improve the window function, many scholars (Moukadem *et al*. 2015, Zidelmal *et al*. 2017) have improved the window function of GST. In this paper, we introduce a new Gaussian window with the following standard deviation

$$\sigma(f)=\frac{1}{m(f+p)^r} \tag{7}$$

The method can describe $\sigma(f)$ through $\{f^r, f^{r-1}, f^{r-2}, \dots\}$. Therefore, the corresponding window function $g(t,f)$ can be expressed as follows

$$g(t,f)=\frac{m(f+p)^r}{\sqrt{2\pi}}e^{\frac{-m^2(f+p)^{2r}t^2}{2}} \tag{8}$$

IGST can be obtained by substituting the improved window function into ST, and the expression of IGST can be shown as follows

$$IGST(\tau,f)=\int_{-\infty}^{+\infty}x(t)\frac{m(f+p)^r}{\sqrt{2\pi}}e^{\frac{-m^2(f+p)^{2r}(t-\tau)^2}{2}}e^{-i2\pi f t}dt \tag{9}$$

The expression of IGST in frequency domain is shown in Eq. (10)

$$IGST(\tau,f)=\int_{-\infty}^{+\infty}H(\alpha+f)\,e^{\frac{-2\pi^2\alpha^2}{m^2(f+p)^{2r}}}e^{i2\pi\alpha\tau}d\alpha \tag{10}$$

2.2 Parameter optimization algorithm

The key problem in GST is how to choose the parameters of the window function, and IGST faces the same problem. In this paper, the energy CM method is used

$$CM(m,p,r)=\frac{1}{\int_{-\infty}^{+\infty}\int_{-\infty}^{+\infty}\left|\overline{IGST_x^{m,p,r}(t,f)}\right|\,dtdf} \tag{11}$$

Normalize the data of IGST

$$\overline{IGST_x^{m,p,r}(t,f)}=\frac{IGST_x^{m,p,r}(t,f)}{\sqrt{\int_{-\infty}^{+\infty}\int_{-\infty}^{+\infty}\left|IGST_x^{m,p,r}(t,f)\right|^2dtdf}} \tag{12}$$

Then, the optimization problem of IGST can be expressed by Eq. (13)

$$\arg\max_{m,p,r}\frac{1}{\int_{-\infty}^{+\infty}\int_{-\infty}^{+\infty}\left|\overline{IGST_x^{m,p,r}(t,f)}\right|\,dtdf} \tag{13}$$

The constraint conditions of the optimization problem are related to the width range of the analyzed window. The window should not be too narrow to change the time resolution, but it should not be too wide to affect the frequency resolution, that is

$$KT_s\le\frac{1}{m(f+p)^r}\le LT_s \tag{14}$$

where, T_s is the sampling period, $f\in[f_{min},\ f_{max}]$, $f_{min}=1$ Hz. In order to satisfy the Nyquist sampling theorem, the value of f_{max} takes half of the sampling frequency. The above formula can be simplified as

$$\begin{cases}KT_s\ m\ (f_{max}+p)^r-1\le 0\\ 1-m\ (1+p)^rLT_s\le 0\end{cases} \tag{15}$$

Refer to related literatures (Moukadem *et al*. 2015, Zidelmal *et al*. 2017), we can let $m\in(0,\ 3]$, $p\in[0,\ 3]$, $r\in[0,\ 1]$, $K=10$ and $L=1000$. The parameters can also be adjusted slightly according to the actual situation.

So, the final optimization problem is as follows

$$\begin{cases} \arg\max\limits_{m,p,r} \dfrac{1}{\int_1^N \int_{f_{min}}^{f_{max}} \left|\overline{IGST_x^{m,p,r}(t,f)}\right|} \\ S_c:\ KT_s m(f_{max}+p)^r - 1 \le 0 \\ \quad 1 - m(1+p)^r LT_s \le 0 \\ \quad 0 < m \le 3 \\ \quad 0 \le p \le 3 \\ \quad 0 \le r \le 1 \end{cases} \tag{16}$$

The above formula can be regarded as the optimization problem of multivariate functions. Under a series of constraints, a set of parameter values are sought to optimize the target value of a certain function or a group of functions. The parameters of IGST window function can be obtained by solving the above problems through optimization algorithm.

2.3 Multi-synchrosqueezing algorithm of IGST

The IF of original signal can be obtained by formula (17)

$$\omega_i(\tau,f) = f + \frac{i\partial_\tau IGST(\tau,f)}{2\pi IGST(\tau,f)} \tag{17}$$

where

$$\partial_\tau IGST(\tau,f) = \frac{\partial IGST(\tau,f)}{\partial\tau} = i2\pi \int_{-\infty}^{+\infty} X(\alpha+f)\,\alpha e^{\frac{-2\pi^2\alpha^2}{m^2(f+p)^{2r}}} e^{i2\pi\alpha\tau} d\alpha \tag{18}$$

Therefore, improved synchrosqueezing generalized S-transform (ISSGST) can be expressed by Eq. (19)

$$ISSGST(\tau,\tilde{f}) = \sum_{f_k:\left|\omega_i(\tau,f_k)-\tilde{f}\right|\le\frac{\Delta f}{2}} |IGST(\tau,f_k)| f_k \tag{19}$$

The expression of IMSSGST is shown in Eq. (20)

$$\begin{aligned} IMSSGST^{[2]}(\tau,\tilde{f}) &= \sum_{f_k:\left|\omega_i(\tau,f_k)-\tilde{f}\right|\le\frac{\Delta f}{2}} \left|IMSSGST^{[1]}(\tau,f_k)\right| f_k \\ IMSSGST^{[3]}(\tau,\tilde{f}) &= \sum_{f_k:\left|\omega_i(\tau,f_k)-\tilde{f}\right|\le\frac{\Delta f}{2}} \left|IMSSGST^{[2]}(\tau,f_k)\right| f_k \\ &\cdots\cdots \\ IMSSGST^{[N]}(\tau,\tilde{f}) &= \sum_{f_k:\left|\omega_i(\tau,f_k)-\tilde{f}\right|\le\frac{\Delta f}{2}} \left|IMSSGST^{[N-1]}(\tau,f_k)\right| f_k \end{aligned} \tag{20}$$

where

$$IMSSGST^{[1]}(\tau,f_k) = ISSGST(\tau,\tilde{f}) \tag{21}$$

3. Frequency-modulated multi-component signal

In order to verify the performance of the proposed method on IF identification, a numerical case of a frequency-modulated multi-component signal is considered. The multi-component signal is defined as Eq. (22)

$$x(t) = x_1(t) + x_2(t) = 2.5\cos(20\pi t + 1.8\sin(1.2\pi t)) + 8\cos(10\pi t + 2\sin(0.8\pi t)) \tag{22}$$

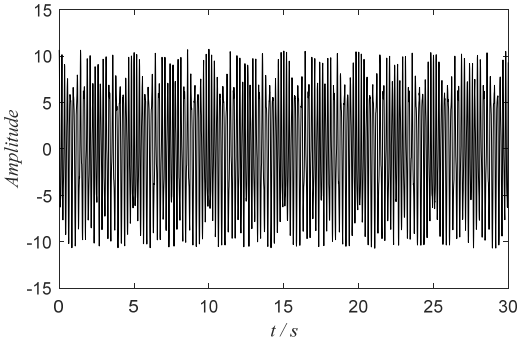

Fig. 1 The simulated multi-component signal with Gaussian white noise

The theoretical frequencies of component signals $x_1(t)$ and $x_2(t)$ are $f_1 = d\,\phi_1 / d\,t = 10 + 1.08\cos(1.2\pi t)$ Hz and $f_2 = d\,\phi_2 / d\,t = 5 + 0.8\cos(0.8\pi t)$ Hz. In this case, the sampling rate is 100 Hz and the sampling time is set to be 30 s. To consider the impact of noise, Gaussian white noise with SNR = 15 dB is added to the signal. The signal after adding white noise is shown in Fig. 1.

The IMSSGST and MSST were performed on the noisy signal. Parameters $m = 3.0489$, $p = 3.0489$ and $r = 0.6901$ are obtained by optimization algorithm for IMSSGST. The results of TFA under one, two and four iterations are presented in Fig. 2 as a representative. It can be seen from Fig. 2 that with the increase of synchrosqueezing time, the energy aggregation of IMSSGST and MSST become higher.

In order to judge the IF identification accuracy of IMSSGST, this paper uses the root mean square value of IF in the time history as the index of accuracy (IA). The smaller the IA value, the closer the recognition value is to the theoretical value.

$$\mathrm{IA} = \frac{\sqrt{\int_0^T [f_d(t) - f_e(t)]^2}}{\sqrt{\int_0^T [f_e(t)]^2}} \tag{23}$$

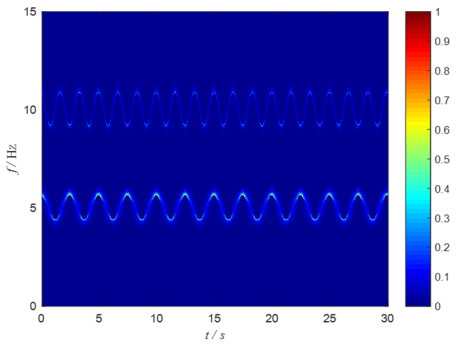

(a) One-synchrosqueezing IGST

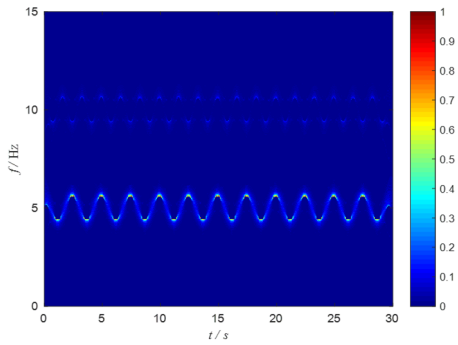

(b) One-synchrosqueezing SST

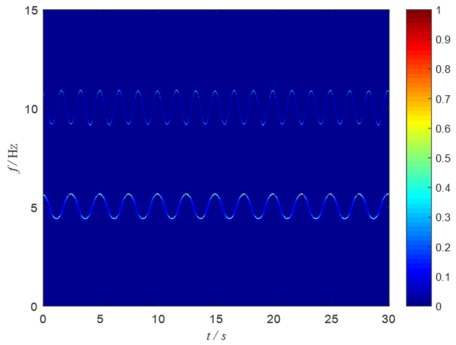

(c) Two-synchrosqueezing IMSSGST

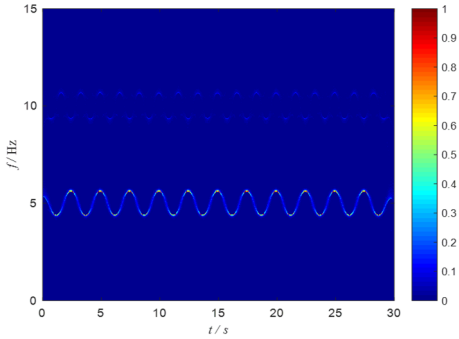

(d) Two-synchrosqueezing MSST

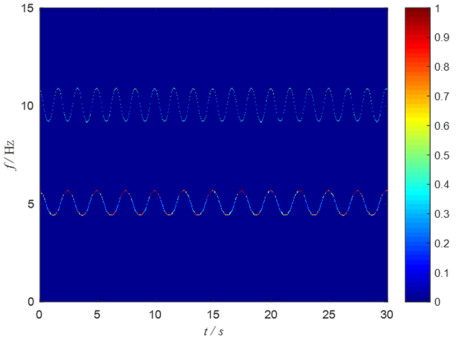

(e) Four-synchrosqueezing IMSSGST

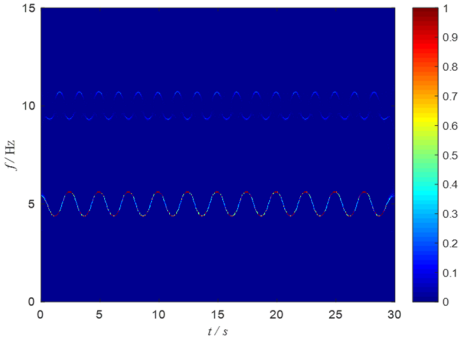

(f) Four-synchrosqueezing MSST

Fig. 2 Results of TFA for the simulated multi-component signal

where, $f_d(t)$ is the identified value of IF, and $f_e(t)$ is the theoretical value of IF.

Table 1 shows the IF identification IA of IMSSGST and MSST methods for the numerical frequency-modulated multi-component signal. IA1 and IA2 represent the IF identification IA of components $x_1(t)$ and $x_2(t)$ respectively. Fig. 3 shows the identification IA values of IMSSGST and MSST under different synchrosqueezing times. It can be seen from Table 1 and Fig. 3 that the identification accuracy of IMSSGST is better than that of MSST under the same synchrosqueezing time. After several iterations, the identification accuracy is tending towards stability. The comparisons between the identified frequencies and the theoretical values are presented in Fig. 4. It is shown that the identified frequencies are in good agreement with their theoretical counterparts. Compared with MSST, the proposed IMSSGST method can extract the IF of each component with higher accuracy.

Table 1 IF identification IA

Index	IMSSGST (%)			MSST (%)		
	One	Two	Four	One	Two	Four
IA_1	2.74	2.44	2.29	3.07	2.65	2.45
IA_2	1.87	1.55	1.51	5.77	4.04	3.62

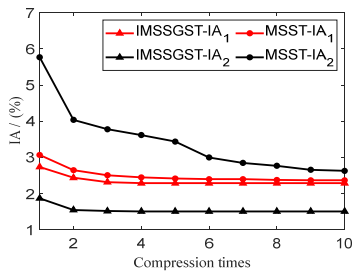

Fig. 3 IA values after different synchrosqueezing times (%)

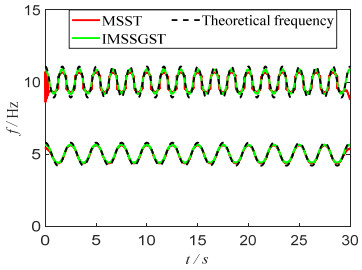

Fig. 4 Results of identified frequency after four-synchrosqueezing

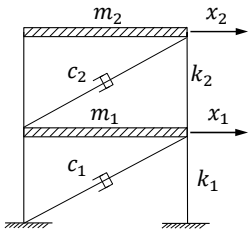

Fig. 5 Two-story shear frame model

Table 2 Parameters of two-layer shear frame model

Layer number	Quality m (kg)	Damping factor c (kN · s/m)	Initial stiffness k (kN/m)
First floor	2.63×10^5	5.47×10^2	3.2×10^5
Second floor	1.74×10^5	1.56×10^2	1.4×10^5

4. Structural IF extraction

4.1 Two-story shear frame model

To verify the feasibility of the proposed method for structural IF identification, a two-story shear frame model as shown in Fig. 5 is established for verification. The corresponding parameters of this structure are shown in Table 2. The time-varying stiffness is shown in Fig. 6, and the theoretical frequency is shown in Fig. 7.

The corresponding equation of motion is

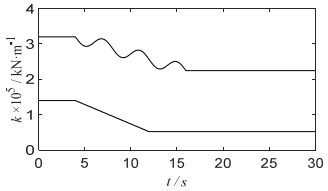

Fig. 6 Structural time-varying stiffness

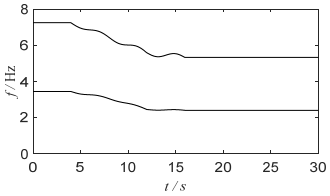

Fig. 7 The theoretical frequency of the structure

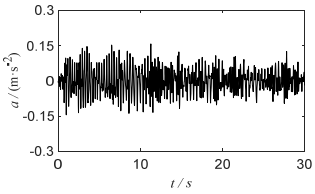

Fig. 8 Acceleration of the first layer under white noise

acceleration responses are obtained by Runge-Kutta method. Among them, the sampling rate is 50 Hz and the sampling time is 30 s. The acceleration response of the first layer under white noise excitation is shown in Fig. 8, and that under EL-Centro earthquake excitation is shown in Fig. 11.

The TFA of the structural acceleration signals of the first layer is carried out, and the IGST parameters are obtained through the optimization algorithm. Among them, $m = 3.0000$, $p = 2.1551$, $r = 0.6454$ is obtained for white noise, and $m = 2.5856$, $p = 1.9398$, $r = 0.6601$ is acquired for EL-Centro earthquake. Figs. 9 and 12 respectively show the time-frequency representations under

$$\begin{cases} m_1\ddot{x}_1 + (c_1 + c_2)\dot{x}_1 - c_2\dot{x}_2 + (k_1 + k_2)x_1 - k_2x_2 = f_1 \\ m_2\ddot{x}_2 - c_2\dot{x}_1 + c_2\dot{x}_2 - k_2x_1 + k_2x_2 = f_2 \end{cases} \tag{24}$$

where, stiffness k_1 and k_2 meet the following conditions

$$k_1 = \begin{cases} 3.2 \times 10^5, & 0 \le t < 4 \\ \left[3.2 - 0.08 \times (t-4) - 0.18 \times sin\left[\frac{\pi}{2}(t-4)\right]\right] \times 10^5, & 4 \le t < 16 \\ 2.2473 \times 10^5, & 16 \le t < 30 \end{cases} \tag{25}$$

$$k_2 = \begin{cases} 1.4 \times 10^5, & 0 \le t < 4 \\ [1.4 - 0.11 \times (t-4)] \times 10^5, & 4 \le t < 12 \\ 0.520 \times 10^5, & 12 \le t < 30 \end{cases} \tag{26}$$

A Gaussian white noise and the 1940 EL-Centro earthquake are used to excite the frame structure respectively, and the structural displacement, velocity and

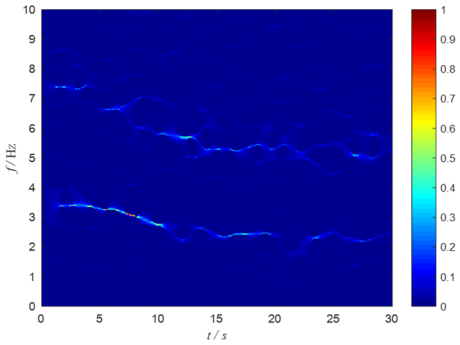

(a) One-synchrosqueezing IGST

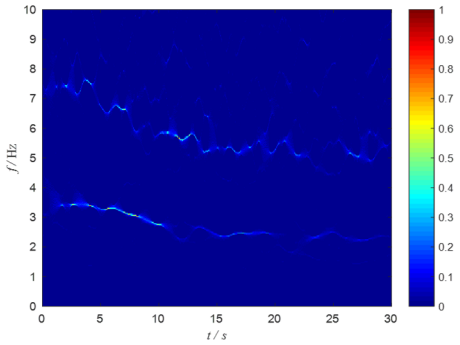

(b) One-synchrosqueezing SST

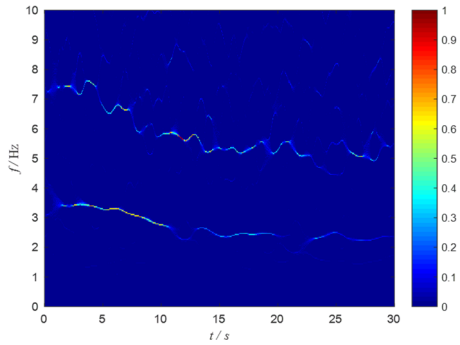

(c) Two-synchrosqueezing IMSSGST

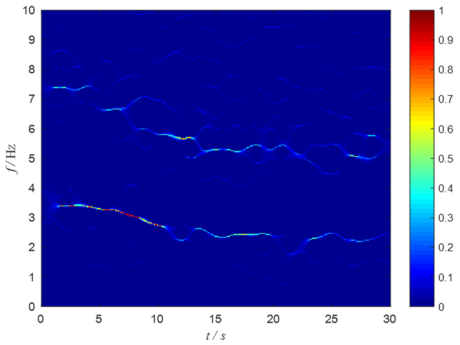

(d) Two-synchrosqueezing MSST

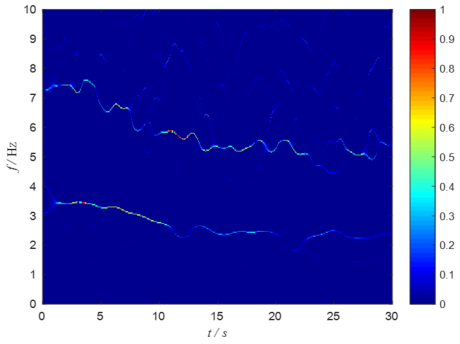

(e) Four-synchrosqueezing IMSSGST

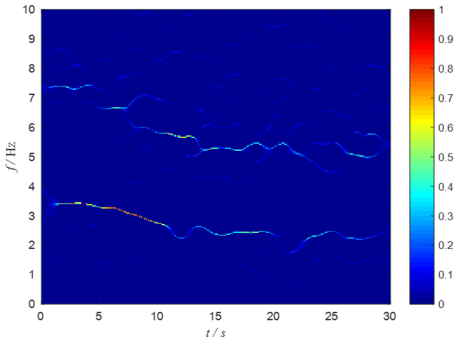

(f) Four-synchrosqueezing MSST

Fig. 9 Results of TFA for the structure under white noise

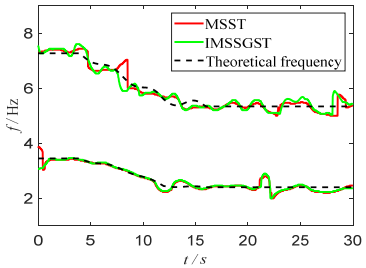

Fig. 10 Results of identified frequency after four-synchrosqueezing white noise

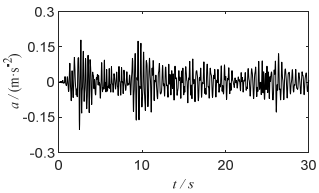

Fig. 11 Acceleration of the first layer under earthquake

white noise excitation and EL-Centro earthquake excitation. Fig. 10 shows the frequency ridge extracted under white noise, and Fig. 13 shows the frequency ridge extracted under EL-Centro earthquake. By comparison, it can be found that the frequency of IMSSGST is smoother and more ideal than that of MSST. To sum up, IMMSGST is also able to perform IF identification of multi-degree freedom structures with varying stiffness, and the results are relatively accurate.

4.2 Three-story steel frame structure

The structure used for the second validation study is the three-story steel frame as shown in Fig. 14. The frame structure adopts 20#a I-steel, whose cross section is shown in Fig. 15. The constitutive model of steel is shown in Fig.

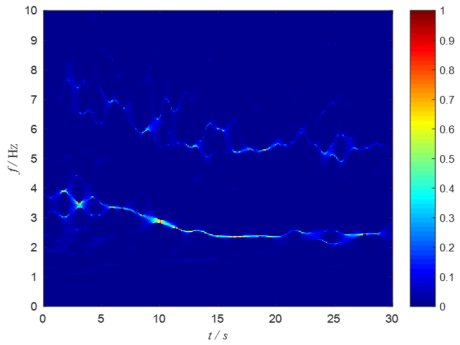

(a) One-synchrosqueezing IGST

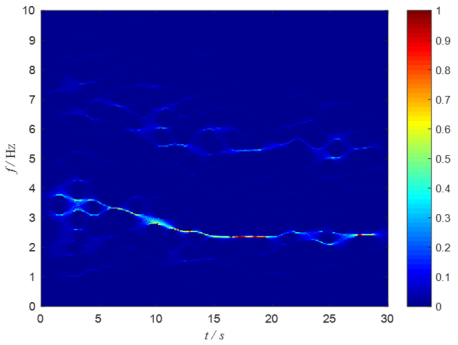

(b) One-synchrosqueezing SST

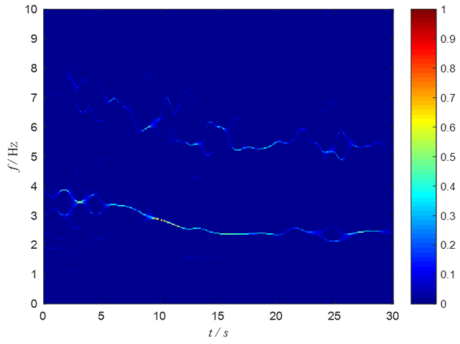

(c) Two-synchrosqueezing IMSSGST

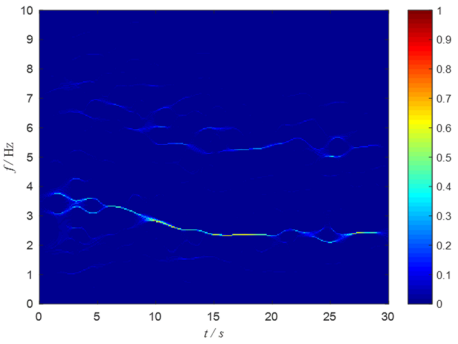

(d) Two-synchrosqueezing MSST

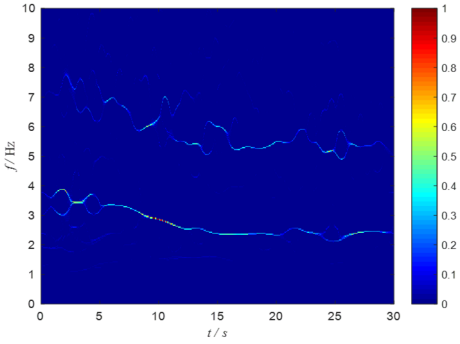

(e) Four-synchrosqueezing IMSSGST

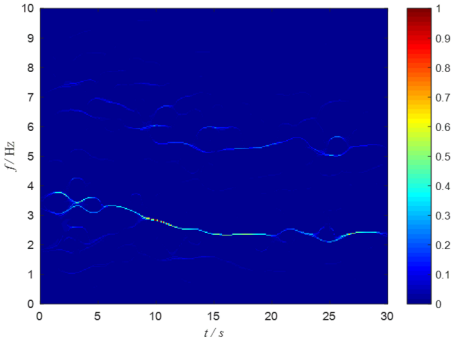

(f) Four-synchrosqueezing MSST

Fig. 12 Results of TFA for the structure under earthquake

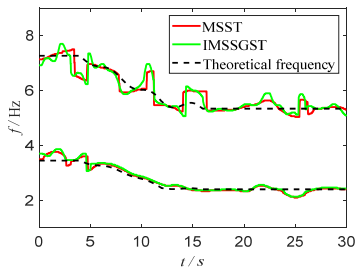

Fig. 13 Results of identified frequency after four-synchrosqueezing under earthquake

16, and the corresponding material properties are yield strength $\sigma_y = 360\,N/mm^2$ and elastic modulus $E = 2 \times 10^5\,Mpa$. The finite element model of this structure is developed in OpenSees using fiber-section displacement-based beam-column elements and the modified Giuffré–Menegotto–Pinto material constitutive model for the structure steel.

Firstly, the frame structure is excited by white noise which is shown in Fig. 17, and the acceleration response of the structure is shown in Fig. 18. IMSSGST and MSST

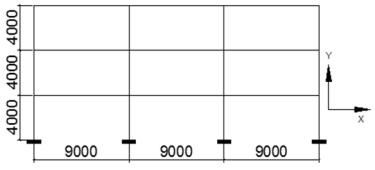

Fig. 14 Details of frame structure

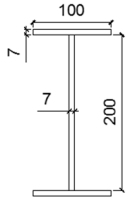

Fig. 15 Section of 20#a I-steel (mm)

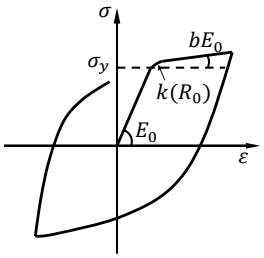

Fig. 16 Constitutive diagram of steel

are used to perform TFA on the structural acceleration response signals, and the synchrosqueezing time are one, two and four respectively. The TFA results are shown in Fig. 19. In IMSSGST, $m = 2.5779$, $p = 1.9386$, $r = 0.6298$ is obtained by optimization algorithm. It can be seen from Fig. 19 that after multi-synchrosqueezing, the aggregation of IMSSGST and MSST time-frequency

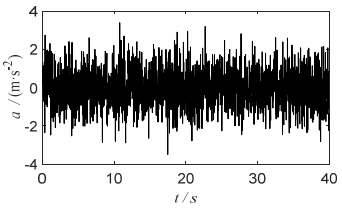

Fig. 17 White noise excitation

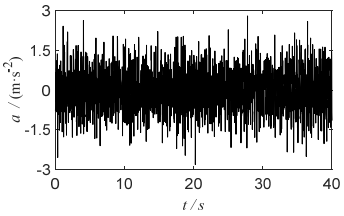

Fig. 18 Structural acceleration response under white noise excitation

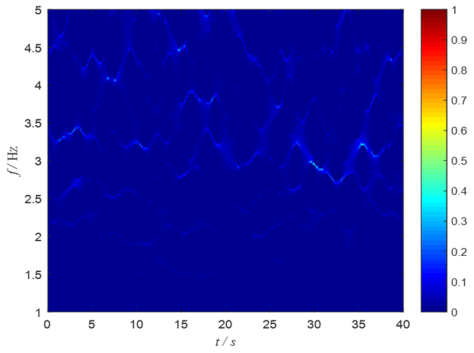

(a) One-synchrosqueezing IGST

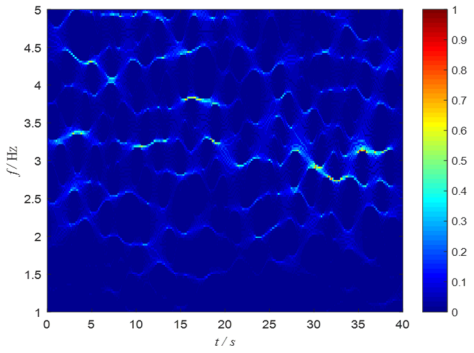

(b) One-synchrosqueezing SST

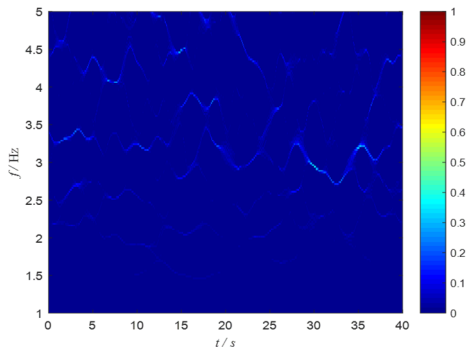

(c) Two-synchrosqueezing IMSSGST

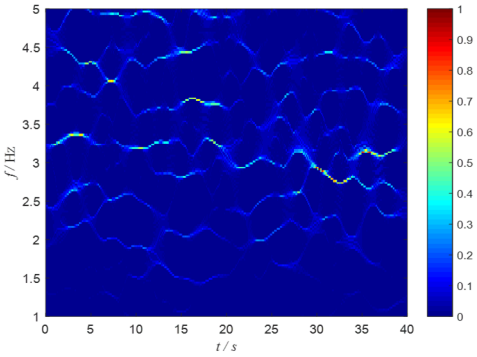

(d) Two-synchrosqueezing MSST

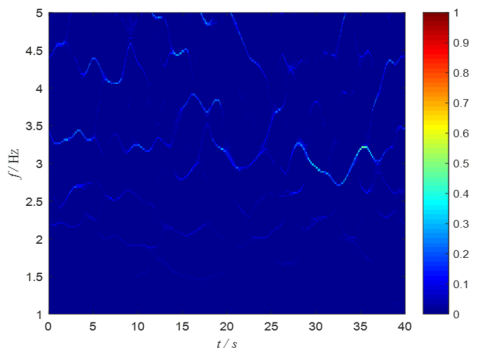

(e) Four-synchrosqueezing IMSSGST

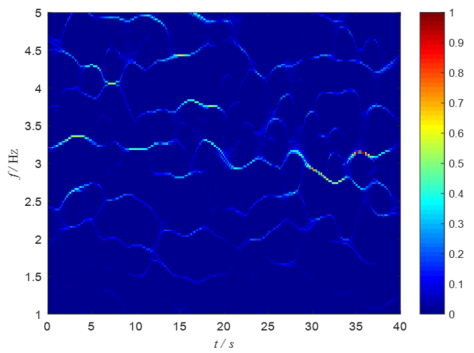

(f) Four-synchrosqueezing MSST

Fig. 19 Results of TFA for the structure under white noise excitation

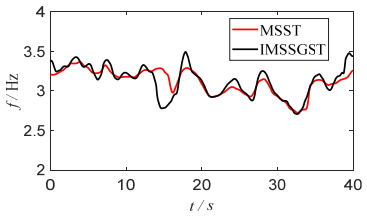

Fig. 20 Identified results under white noise excitation

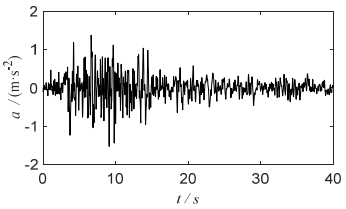

Fig. 21 Taft earthquake excitation

ridges is obviously improved, but the anti-noise performance of MSST is still weak. The frequency after four-synchrosqueezing is extracted, and the result is shown in Fig. 20. It can be seen from this figure that due to the complex material constitutive model and hysteresis mode in simulation, the frequency curve of the proposed method may seem more unstable than that of MSST. However, both IMSSGST and MSST can effectively identify frequency of the frame structure after multiple compression, and they are

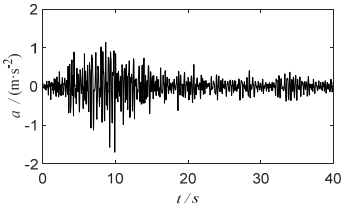

Fig. 22 Structural acceleration response under Taft earthquake excitation

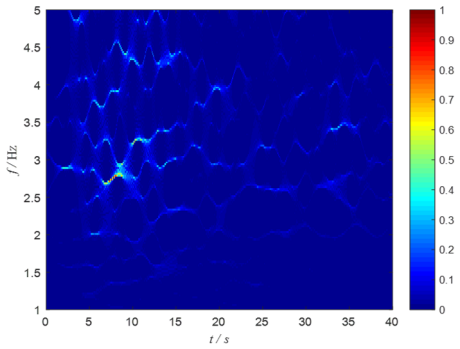

(a) One-synchrosqueezing IGST

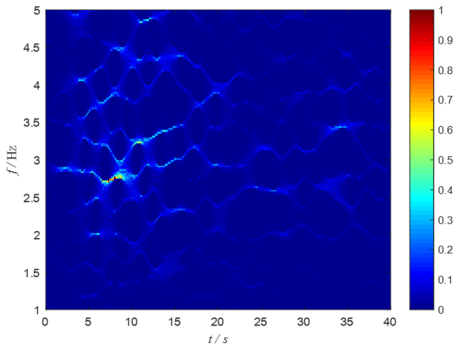

(b) One-synchrosqueezing SST

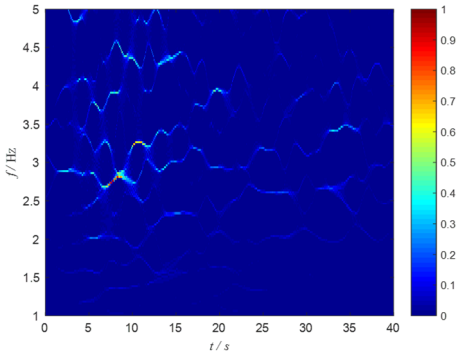

(c) Two-synchrosqueezing IMSSGST

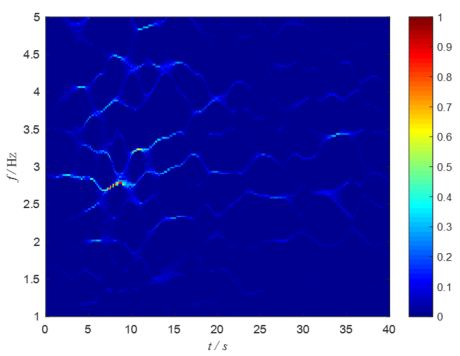

(d) Two-synchrosqueezing MSST

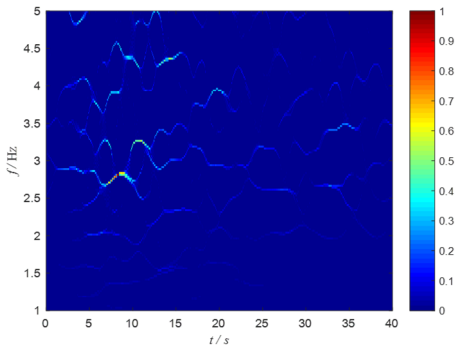

(e) Four-synchrosqueezing IMSSGST

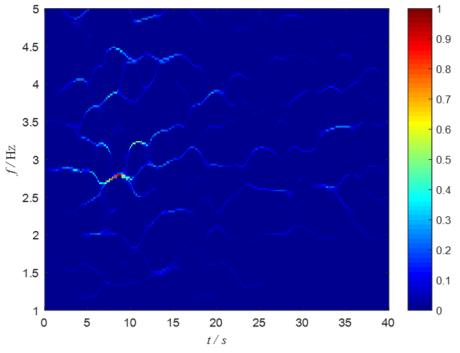

(f) Four-synchrosqueezing MSST

Fig. 23 Results of TFA for the structure under Taft earthquake excitation

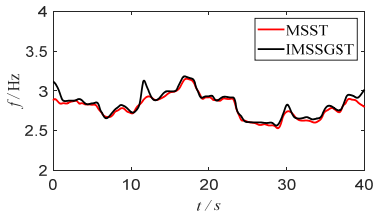

Fig. 24 Identified results under Taft earthquake excitation

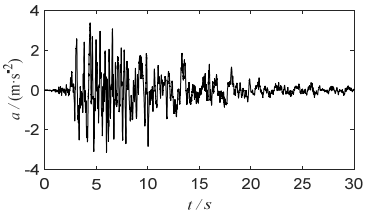

Fig. 25 Earthquake excitation applied to the shear wall

basically consistent. The instantaneous frequency trend is correct and the identification accuracy is acceptable.

In order to further explore the practicability and accuracy of IMSSGST, the three-story frame structure under Taft earthquake excitation is analyzed again. The excitation is shown in Fig. 21 and the acceleration response of the structure is shown in Fig. 22. The acceleration response is analyzed by the same TFA method, and the parameter$m = 3.0000$, $p = 2.1860$, $r = 0.5727$ in IGST is obtained by optimization algorithm. Fig. 23 shows the

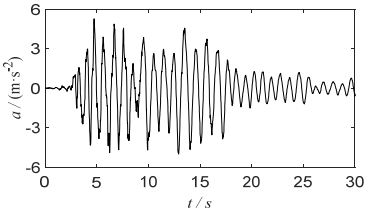

Fig. 26 Acceleration response of the shear wall

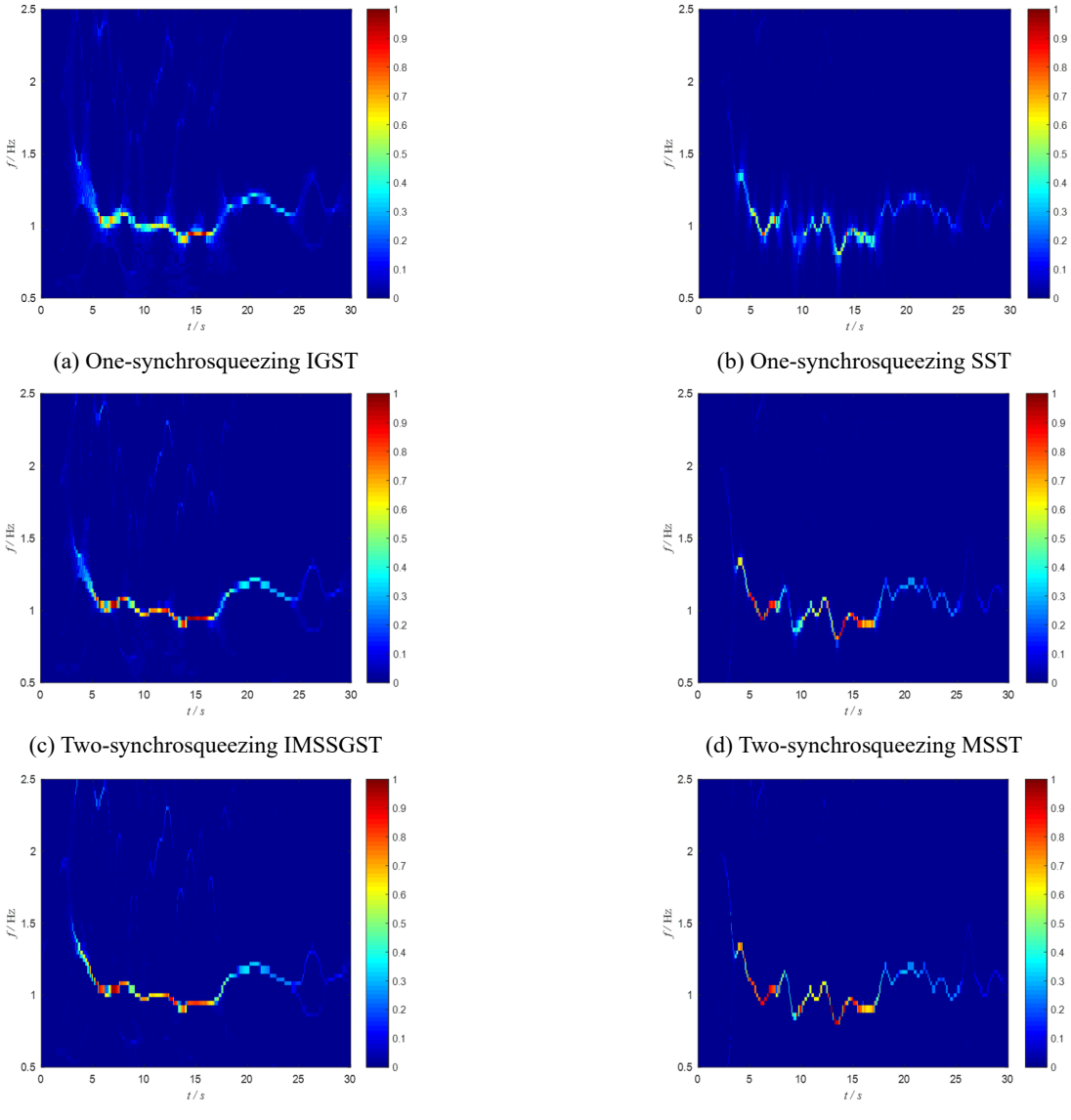

(a) One-synchrosqueezing IGST

(b) One-synchrosqueezing SST

(c) Two-synchrosqueezing IMSSGST

(d) Two-synchrosqueezing MSST

(e) Four-synchrosqueezing IMSSGST

(f) Four-synchrosqueezing MSST

Fig. 27 Results of TFA for the shear wall under earthquake excitation

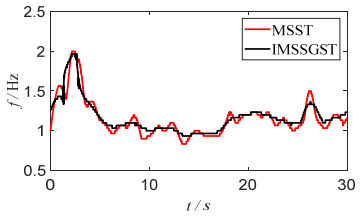

Fig. 28 Identified results under earthquake excitation

results of TFA. The results of frequency extraction after four-synchrosqueezing are shown in Fig. 24. It is obvious that IMSSGST can accurately identify the IF of the structure, which shows that IMSSGST is a practical TFA method.

5. Experimental study

In order to verify the IF identification performance of IMSSGST on actual structures, the test data of a seven-story RC shear wall designed by Panagiotou *et al*. (2011) of University of California, San Diego (USCD-NEES) are analyzed. The Earthquake excitation applied to the structure is shown in Fig. 25, and the acceleration response of RC shear wall is shown in Fig. 26.

IMSSGST and MSST are used to perform TFA on the measured acceleration response signals, and the TFA results are shown in Fig. 27. In IMSSGST, $m = 1.3469$, $p = 3$, $r = 0.9170$ is obtained by optimization algorithm. It can be seen from Fig. 27 that with the increase of synchrosqueezing times, the frequency ridges identified by IMSSGST and MSST are more and more accurate and obvious. Under the same synchrosqueezing times, compared with MSST, the frequency curve identified by IMSSGST fluctuates less, which is beneficial to extract the IF of the structure. The instantaneous frequencies of IMSSGST and MSST after four-synchrosqueezing are extracted by extreme value method. The frequency extraction results are shown in Fig. 28. It can be seen from this figure that the frequency response range of the RC shear wall structure under earthquake excitation is 0.8~2.1 Hz, and both IMSSGST and MSST can effectively identify the frequency range, but the IF curve identified by IMSSGST is smoother and the curve fluctuation is smaller.

6. Conclusions

In this paper, by combining a new form of IGST and MSST operation, the IMSSGST is proposed and applied to identify the IF of time-varying and nonlinear structures. The numerical simulation and experimental results show that:

- By combining CM principle with parameter optimization algorithm, the parameters of adjustment factors in IGST can be quickly obtained, and the calculation accuracy is significantly improved.
- After multi-synchrosqueezing, the time-frequency energy is more concentrated, which can effectively improve the frequency identification accuracy of IMSSGST.
- Compared with MSST algorithm, the frequency curve identified by IMSSGST is smoother, and the curve fluctuation is smaller. So IMSSGST is an accurate and efficient TFA method.

Acknowledgments

Financial support to complete this study is provided in part by the National Natural Science Foundation of China (Grant No. 51979130), Natural Science Research of Jiangsu Higher Education Institutions of China (Grant No. 20KJB560016), and Foundation of Jiangsu University of Science and Technology (Grant No. 1122931804). The results and opinions expressed in this paper are those of the authors only and they don't necessarily represent those of the sponsors.

References

Assous, S. and Boashash, B. (2012), "Evaluation of the modified S-transform for time-frequency synchrony analysis and source localization", *Eurasip J. Adv. Signal Process*, **2012**, 49. https://doi.org/10.1186/1687-6180-2012-49

Behera, R., Meignen, S. and Oberlin, T. (2018), "Theoretical analysis of second-order synchrosqueezing transform", *Appl. Comput. Harmon. Anal.*, **45**(2), 379-404. https://doi.org/10.1016/j.acha.2016.11.001

Cao, H., Xi, S., Chen, X. and Wang, S. (2016), "Zoom synchrosqueezing transform and iterative demodulation: Methods with application", *Mech. Syst. Signal Pr.*, **72-73**, 695-711. https://doi.org/10.1016/j.ymssp.2015.11.030

Daubechies, I., Lu, J.F. and Wu, H.T. (2011), "Synchrosqueezed wavelet transforms: An empirical mode decomposition decomposition-like tool", *Appl. Comput. Harmon. A.*, **30**(2), 243-261. https://doi.org/10.1016/j.acha.2010.08.002

Djurović, I., Sejdić, E. and Jiang, J. (2008), "Frequency-based window width optimization for S-transform", *AEU-Int. J. Electron. C.*, **62**, 245-250. https://doi.org/10.1016/j.aeue.2007.03.014

Feng, Z., Chen, X. and Liang, M. (2015), "Iterative generalized synchrosqueezing transform for fault diagnosis of wind turbine planetary gearbox under nonstationary conditions", *Mech. Syst. Signal Pr.*, **52**, 360-375. https://doi.org/10.1016/j.ymssp.2014.07.009

Guo, S.X. and Pei, Q. (2017), "Application of short-time Fourier transform to high-rise frame structural-health monitoring based on change of inherent frequency over time", *J. Chongqing Univ. (English Edition)*,**16**(01), 1-10.

Hou, Z., Hera, A. and Shinde, A. (2010), "Wavelet-based structural health monitoring of earthquake excited structures", *Comput-Aided Civ. Inf.*, **21**(4), 268-279. https://doi.org/10.1111/j.1467-8667.2006.00434.x

Kang, J.X. (2018), "Research on improved synchroextracting transform and its application in seismic signal processing", *ChengDu University of Technology*.

Kijewski, T. and Kareem, A. (2010), "Wavelet transforms for system identification in civil engineering", *Comput.-Aid. Civ. Inf.*, **18**(5), 339-355. https://doi.org/10.1111/1467-8667.t01-1-00312

Le, T.P. and Argoul, P. (2015), "Distinction between harmonic and structural components in ambient excitation tests using the time–frequency domain decomposition technique", *Mech. Syst. Signal Pr.*, **52-53**, 29-45.

https://doi.org/10.1016/j.ymssp.2014.07.008
Lei, Y., Lin, J., He, Z., and Zuo, M.J. (2013), "A review on empirical mode decomposition in fault diagnosis of rotating machinery", *Mech. Syst. Signal Pr.*, **35**, 108-126. https://doi.org/10.1016/j.ymssp.2012.09.015
Li, C. and Liang, M. (2012), "A generalized synchrosqueezing transform for enhancing signal time time-frequency representation", *Signal Process.*, **92**(9), 2264-2274. https://doi.org/10.1016/j.sigpro.2012.02.019
Li, Z., Gao, J., Wang, Z., Liu, N. and Yang, Y. (2020), "Time-synchroextracting general Chirplet transform for seismic time-frequency analysis", *IEEE Trans. Geosci. Remote Sens.*, **58**(12), 8626-8636. https://doi.org/10.1109/TGRS.2020.2989403
Liu, J.L., Wang, Z.C., Ren, W.X. and Li, X.X. (2015), "Structural time-varying damage detection using synchrosqueezing wavelet transform", *Smart Struct. Syst., Int. J.*, **15**(1), 119-133. https://doi.org/10.12989/sss.2015.15.1.119
Liu, N., Gao, J., Zhang, B., Li, F. and Wang, Q. (2017a), "Time–frequency analysis of seismic data using a three parameters S transform", *IEEE Geosci. Remote S.*, **15**(1), 142-146. https://doi.org/10.1109/LGRS.2017.2778045
Liu, N., Gao, J., Zhang, Z., Jiang, X. and Lv, Q. (2017b), "High-resolution characterization of geologic structures using the synchrosqueezing transform", *Interpret.-J. Sub.*, **5**(1), 75-85. https://doi.org/10.1190/INT-2016-0006.1
Liu, J.L., Wei, X.J., Qiu, R.H., Zheng, J.Y., Zhu, Y.J. and Irwanda, L. (2018a), "Instantaneous frequency extraction in time-varying structures using a maximum gradient method", *Smart Struct. Syst., Int. J.*, **22**(3), 359-368. https://doi.org/10.12989/sss.2018.22.3.359
Liu, N., Gao, J., Jiang, X., Zhang, Z. and Wang, P. (2018b), "Seismic instantaneous frequency extraction based on the SST-MAW", *J. Geophys. Eng.*, **15**(3), 995-1007. https://doi.org/10.1088/1742-2140/aa8cb6
Liu, N., Gao, J., Zhang, B., Wang, Q. and Jiang, X. (2019), "Self-adaptive generalized S-transform and its application in seismic time–frequency analysis", *IEEE Geosci. Remote S.*, **57**(10), 7849-7859. https://doi.org/100.1109/TGRS.2019.2916792
Moukadem, A., Bouguila, Z., Ould-Abdeslam, D. and Dieterlen, A. (2015), "A new optimized Stockwell transform applied on synthetic and real non-stationary signals", *Digit. Signal Process.*, **46**, 226-238. https://doi.org/10.1016/j.dsp.2015.07.003
Ni, S.H., Yang, Y.Z. and Tsai, P.H. (2017), "Evaluation of pile defects using complex continuous wavelet transform analysis", *NDT&E Int.*, **87**, 50-59. https://doi.org/10.1016/j.ndteint.2017.01.007
Oberlin, T., Meignen, S. and Perrier, V. (2015), "Second-order synchrosqueezing transform or invertible reassignment? Towards ideal time time-frequency representations", *IEEE T. Signal Process.*, **63**(5), 1335-1344. https://doi.org/10.1109/TSP.2015.2391077
Panagiotou, M., Restrepo, José, I. and Conte, J.P. (2011), "Shake-table test of a full-scale 7-story building slice. Phase I: Rectangular wall", *J. Struct. Eng.*, **137**(6), 691-704. https://doi.org/10.1061/(ASCE)ST.1943-541X.0000332
Patil, D.O. and Hamde, S.T. (2021), "Automated detection of brain tumor disease using empirical wavelet transform based LBP variants and ant-lion optimization", *Multimed. Tools Appl.*, **80**, 17955-17982. https://doi.org/10.1007/s11042-020-10434-2
Pham, D.H. and Meignen, S. (2017), "High-order synchrosqueezing transform for multicomponent signals analysis-with an application to gravitational gravitational-wave signal", *IEEE T. Signal Process.*, **65**(12), 3168-3177. https://doi.org/10.1109/TSP.2017.2686355
Pinnergar, C.R. and Mansinha, L. (2003), "The S-transform with windows of arbitrary and varying shape", *Geophysics*, **68**, 381-385. https://doi.org/10.1190/1.1543223
Sanchez, W.D., Brito, J.V.D. and Avila, S.M. (2020), "Structural health monitoring using synchrosqueezed wavelet transform on IASC-ASCE benchmark phase I", *Int. J. Struct. Stab. Dyn.*, **20**(12), 2050138. https://doi.org/10.1142/S0219455420501382
Stanković, L. (2001), "A measure of some time–frequency distributions concentration", *Signal Process.*, **81**(3), 621-631. https://doi.org/10.1016/S0165-1684(00)00236-X
Thakur, G. and Wu, H.T. (2011), "Synchrosqueezing-based recovery of instantaneous frequency from nonuniform samples", *SIAM J. Math. Anal.*, **43**(5), 2078-2095. https://doi.org/10.1137/100798818
Wang, Z.C., Ren, W.X. and Chen, G.D. (2018), "Time-frequency analysis and applications in time-varying/nonlinear structural systems: A state-of-the-art review", *Adv. Struct. Eng.*, **21**(10), 1562-1584. https://doi.org/10.1177/1369433217751969
Xu, X.Z., Zhang, Z.Y., Hua, H.X. and Chen, Z.N. (2003), "Identification of time-varying modal parameters by a linear time-frequency method", *J. Vib. Eng.*, **3**, 104-108.
Yu, G., Yu, M. and Xu, C. (2017), "Synchroextracting transform", *IEEE T. Ind. Electron.*, **64**(10), 8042-8054.
Zhang, Z.Y., Liu, Y.X. and Li, X.Y. (2018), "Extracting instantaneous attributes of seismic signals with synchrosqueezing wavelet transform", *Comput. Measur. Control*, **26**(10), 260-263.
Zhang, W.H., Hu, M.H., Jiang, Z.N. and Feng, K. (2020), "Order tracking method for gas turbine combined with synchroextracting transform and Vold-Kalman filtering", *J. Mech. Electr. Eng.*, **37**(09), 1104-1108.
Zheng, J., Pan, H., Yang, S. and Cheng, J. (2017), "Adaptive parameterless empirical wavelet transform based time time-frequency analysis method and its application to rotor rubbing fault diagnosis", *Signal Process Process.*, **130**, 305-314. https://doi.org/10.1016/j.sigpro.2016.07.023
Zidelmal, Z., Hamil, H., Moukadem, A., Amirou, A. and Ould-Abdeslam, D. (2017), "S-transform based on compact support kernel", *Digit. Signal Process.*, **62**, 137-149. https://doi.org/10.1016/j.dsp.2016.11.008

HJ